Theor Chem Acc (1999) 102:366–376
DOI 10.1007/s00214980m146

Theoretical
Chemistry Accounts

Regular article

The catalyzed hydrosilation reaction: substituent effects*

Brett M. Bode, Mark S. Gordon

Department of Chemistry, Iowa State University, Ames, IA 50011, USA

Received: 11 August 1998 / Accepted: 3 September 1998 / Published online: 23 February 1999

Abstract. Ab initio electronic structure calculations using MP2 wavefunctions have been used to investigate a reaction path for the hydrosilation reaction catalyzed by divalent titanium [modeled by TiH_2, $TiCl_2$, and $Ti(C_5H_5)_2$]. Optimized structures and energies are presented. All model reactions predict a barrierless reaction path compared to a barrier of 78 kcal/mol for the uncatalyzed reaction.

Key words: Hydrosilation – CCSD(T) – Substituent effects – MP2 – Titanium catalysts

1 Introduction

The hydrosilation reaction is a general method for adding an Si—H bond across a C—C double bond. This method encompasses a wide variety of substituted alkenes, dienes, and alkynes, leading to many different organosilicon products. Thus the method is very useful; indeed, it is the second most important method of producing organosilanes on a large scale [1]. The general hydrosilation reaction may be written as:

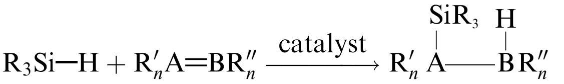

$$R_3Si{-}H + R'_nA{=}BR''_n \xrightarrow{\text{catalyst}} R'_n\overset{SiR_3}{\overset{|}{A}}{-\!\!-}\overset{H}{\overset{|}{B}}R''_n \qquad (1)$$

One of the simplest examples known experimentally is the addition of trichlorosilane to ethylene, which will occur rapidly at room temperature and give nearly 100% yields with a variety of homogeneous transition-metal-based catalysts [2].

Several analogous uncatalyzed reactions ($HSiCl_3$, SiH_4 + ethylene, SiH_4 + propene) were studied previously [3]; all were found to have large (≥54 kcal/mol) barriers. Thus, the catalyst is crucial in making the process economically viable. Industrially, one active catalyst is believed to be a divalent $TiCp_2$ species ($Cp = C_5H_5$).The role of $TiCp_2$ in catalyzing the polymerization of primary organosilanes has been studied by Harrod et al. [4]. These calculations suggest that $TiCp_2$ exhibits a strong catalytic effect, but owing to the size of the catalyst only selected points along the reaction path were studied in detail using double-ζ and triple-ζ quality basis sets and density functional theory. The nature of the bridging interactions between Ti and C in $Ti\{C(SiMe_3){=}C(Ph)(Me)\}(Cp)_2^+$, an intermediate in a Ziegler catalyst system, has also been examined. The computed structure matched the experimental structure very well, even though the calculations employed fairly low levels of theory (RHF wavefunctions with a 3-21G basis set) [5].

There have been several recent studies on similar catalysts. A study of a silylene-bridged $TiCp_2$ and its role in ethylene polymerization [6] employed RHF, MP2, and QCISD calculations with small basis sets (effective core potentials on the metal and 3-21G on the carbons and hydrogens). The results give a qualitative picture of the reaction path and several important structures along it, but the entire path was not examined. The Ziegler-Natta olefin polymerization process has been studied by several groups interested in the role of the $TiCl_2$ catalyst [7–9]. Similar structures were also found in a study of the McMurry reaction involving the $TiCl_2$-catalyzed reductive coupling of carbonyl compounds [10]. While these studies do provide a qualitative picture of the process, they all use relatively small basis sets and modest levels of theory (RHF and MP2).

In a previous paper [11] we considered the simplest prototypical example of a catalyzed hydrosilation reaction (Eq. 1), in which A and B are carbon, R, R′, and R″ are hydrogen, and the catalyst is TiH_2. The choice of reactants and catalyst allowed mapping the entire reaction path at a high level of theory [MP2 geometries plus CCSD(T) energetics]. From this baseline work it was determined that the MP2 level of theory was adequate to determine both the reaction energies and the optimized geometries. Preliminary calculations on the effect of Cl substitution on the hydrosilation reaction have recently been reported [12].

---

* Contribution to the Kenichi Fukui Memorial Issue

Correspondence to: M.S. Gordon

In this paper, we will examine the similarities and differences between the model system in our previous work and the actual experimental systems: the reaction studied will be ethylene + trichlorosilane, the simplest experimental system. The catalysts will include the model catalyst from our previous work, TiH_2, the catalyst used in model studies of many similar reactions, $TiCl_2$, and finally the catalyst believed to be involved in the experimental reaction system, $TiCp_2$.

2 Computational methods

In our previous work the minimum energy reaction path connecting reactants to products was determined using all-electron ab initio wavefunctions with a basis set of triple-ζ plus polarization quality. To examine the effects of substituents we required a more computationally efficient basis set capable of similar accuracy to our previous work.

We first tried using an SBKJC effective core potential (ECP) [13] basis on C, Si, Cl, and Ti and a 6-31 G(*p*) basis set on hydrogen. The SBKJC basis set was extended with one *d*-type polarization function on each C, Si, and Cl [14]. This basis set was evaluated by reoptimizing the stationary points in the reaction path from our previous work. As shown in Fig. 1, the SBKJC basis set tracks the triple-ζ basis, but it overestimates the exothermicity by 7–8 kcal/mol over most of the reaction path, leading to an rms deviation of 6.7 kcal/mol. However, it was found that the rms difference drops to 0.5 kcal/mol when the C ECP basis set is replaced with a 6-31 G(*d*) basis set (see Fig. 1). Thus we have used a 6-31 G(*d,p*) [15] basis set on H and C, and the SBKJC ECP basis on Si, Cl, and Ti extended with one *d*-type polarization function on Si and Cl.

All calculations were performed using closed-shell Møller-Plesset second-order perturbation theory (MP2) as implemented in the GAMESS [16] program. The reaction paths involving TiH_2 and $TiCl_2$ were determined by first optimizing the structures of the minima and transition states (TS) using analytic gradients and a modified Newton-Raphson algorithm. Each stationary point was confirmed by computing the matrix of energy second derivatives (hessian), to obtain the harmonic normal modes and corresponding frequencies (each minimum has zero and each transition state has one imaginary mode). The calculated frequencies also provide the harmonic zero-point energies used to convert energy differences to 0 K enthalpy differences. Finally, the path connecting each TS to the nearest minimum on each side of the TS was computed using the Gonzalez-Schlegel second-order intrinsic reaction coordinate path (IRC) method [17] with a step size 0.3 $amu^{1/2}$ bohr for the first TS and 0.05 $amu^{1/2}$ bohr for the second TS. For the reaction path involving $TiCp_2$, selected stationary points were reoptimized as noted above. The TS was also confirmed by computing its hessian. Owing to the high computational cost of the large $TiCp_2$ reaction system, hessians, and thus ZPE corrections, were not performed on the minima.

3 Results and discussion

Figure 2 shows the energy profile of each of the reaction systems. The zero of energy on the curve for each reaction is the sum of the reactant energies (structures **a, b,** and **c**) for that reaction. The MP2 structures at each unique stationary point are given separately for the catalysts TiH_2, $TiCl_2$, and $TiCp_2$ in Figs. 3, 4, and 5, respectively [18]. Animations of the IRCs shown in Fig. 2 are available in the Appendix [19]. Structures that are identical for all three reactions, structures **b, c,** and **o,** are shown only in Fig. 3. The MP2 total energies and the MP2 vibrational zero point energy (ZPE) corrections for each geometry point marked in Figs. 2–5 are available in the Appendix. MP2 ZPE corrected energies are listed relative to the zero of energy in Table 1. Note that MP2 ZPE corrections were not performed on many of the geometries involving $TiCP_2$ owing to the high computational cost.

It is important to note that all points on the energy plot in Fig. 2 lie below the energy of the reactants, in contrast to the large barrier in the uncatalyzed reactions. In addition, all three reaction systems in the current study exhibit quite similar stationary points, although

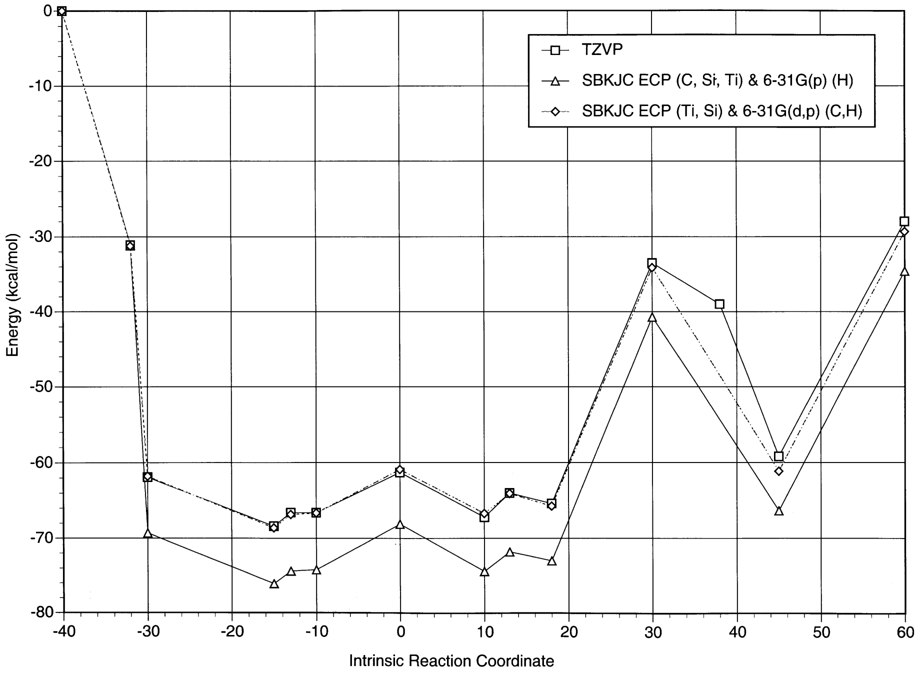

Fig. 1. Comparison of TZVP versus SBK ECP basis sets

Fig. 2. MP2 reaction energy profiles

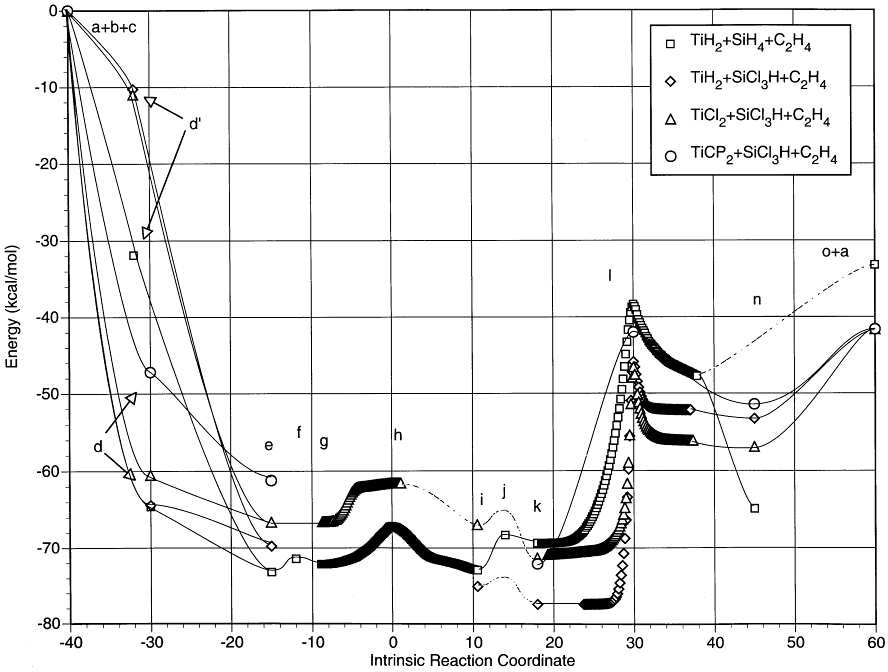

there are some differences in the energetics of the reactions. The following text will lay out the reaction in detail for $TiCl_2$, shown in Fig. 4, noting the differences in the TiH_2 and $TiCp_2$ reactions where appropriate.

There are two possibilities for the first step of the reaction, both of which are barrierless processes. The first, and more exothermic, is to add the catalyst across the ethylene double bond to form the three-membered ring compound shown in **d** (Fig. 4). This process is downhill in energy by 59.6 kcal/mol at the ZPE corrected MP2 level of theory. Note that, based on the large exothermicity and the large (0.15 Å) increase in the C—C bond length, structure **d** is a three-membered ring, not a π complex. Silane will then add to form the complex depicted in **e**. This second barrierless addition is downhill by 5.3 kcal/mol.

In our previous work [11] we found an alternative pathway, with TiH_2 adding to SiH_4 first. This addition resulted in a Ti insertion into an Si—H bond. However, the subsequent addition of C_2H_4 resulted in a barrierless rearrangement to structure **e**. In the present study, using $SiCl_3H$ instead of SiH_4, neither $TiCl_2$ nor TiH_2 inserted into the Si—H bond. Instead, a simple complex is formed as shown in structure **d′**. Since there is no insertion, the addition of $SiCl_3H$ to $TiCl_2$ (or TiH_2) is much less exothermic than the addition of SiH_4 (10.6 kcal/mol versus 31.1 kcal/mol). Just as in the previous work, once C_2H_4 is added the complex spontaneously rearranges to structure **e**. Since neither $TiCl_2$ nor TiH_2 inserted into the Si—H bond, it is unlikely that $TiCp_2$ would insert. Thus an optimization of a structure similar to **d′** using $TiCp_2$ was not attempted.

The net result after the two reactants and the catalyst have been added together is the formation of compound **e**, with no intervening barrier in either of the two possible routes. The overall exothermicity to this point is more than 60 kcal/mol in all the systems studied, driven predominately by the addition of the catalyst to ethylene. This very large drop in energy drives the entire reaction path down in energy. In fact, the reaction path is forced down enough that all subsequent points are below the reactants in energy.

Recall that the final desired product is ethyltrichlorosilane. So, starting from compound **e** in Fig. 4, the silyl group needs to migrate to the nearest (α) carbon, and a hydrogen needs to be transferred to the adjacent (β) carbon, with the ultimate removal of the catalyst. Therefore, the next step in the reaction is to transfer a H from the complexed silane to the Ti and to attach the Si to the α-C.

In our previous study it was found that the system went through a small barrier to a structure **g** (not shown here) which has the silane rotated such that there are two bridging hydrogens. However, the small barrier went to zero when ZPE corrections were added. For $SiCl_3H$, a similar minimum would have one bridging hydrogen and one bridging chlorine. However, no such minimum could be found for any of the catalysts studied. Thus, it is likely that the TS represented by a structure **f** in the previous study (not shown here) simply does not exist for the reaction involving $SiCl_3H$.

In the model system studied previously a small (5.3 kcal/mol) barrier was found which connected structure **e** (through structure **g**) to structure **i**. For reaction **III** a similar TS, shown as **h** in Fig. 4, has been located 6.3 kcal/mol in energy above structure **e**. The IRCs from the TS are shown in Fig. 2. They illustrate the extreme flatness of the surface in the TS region, which is the reason the correct TS is so difficult to locate. The IRC leading towards the products for structure **h** stops after 11 steps and after lowering the energy by 0.006 kcal/mol, due to a very small gradient. Optimizations from the end of the IRC show that there might be two possible results of this step. The first is the desired

Fig. 3. MP2 structures along the minimum energy reaction path

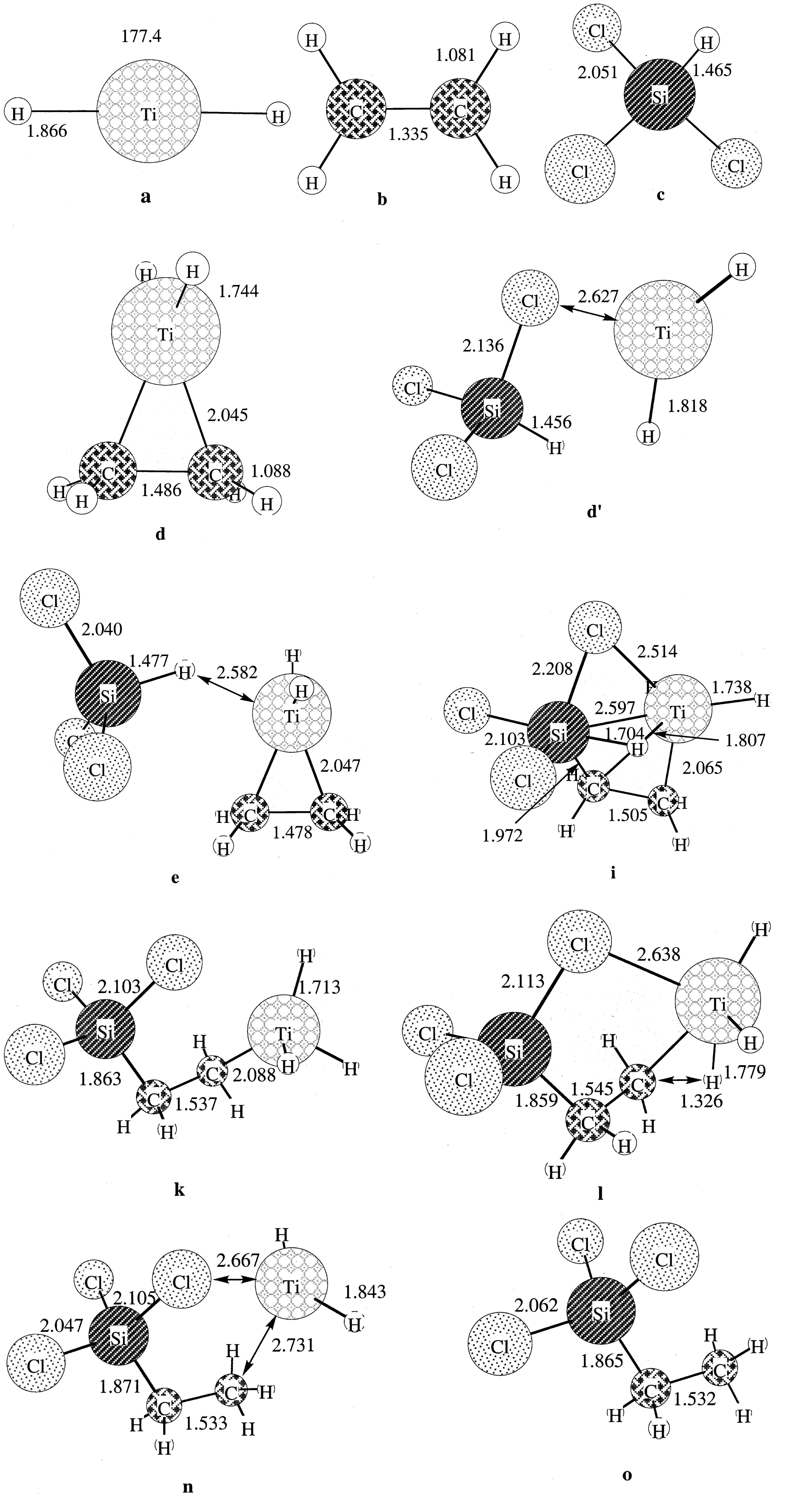

Fig. 4. MP2 structures along the minimum energy reaction path using $TiCl_2$ as the catalyst

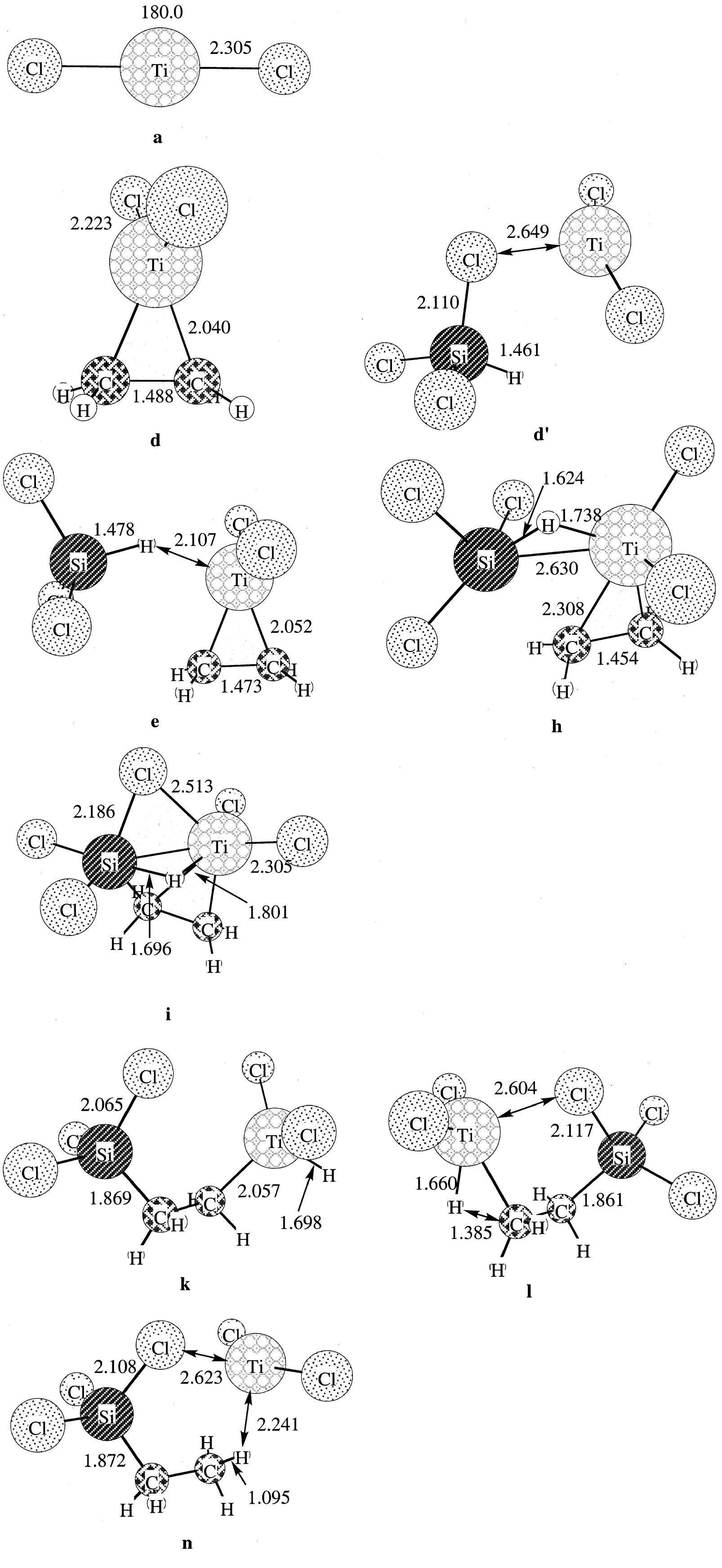

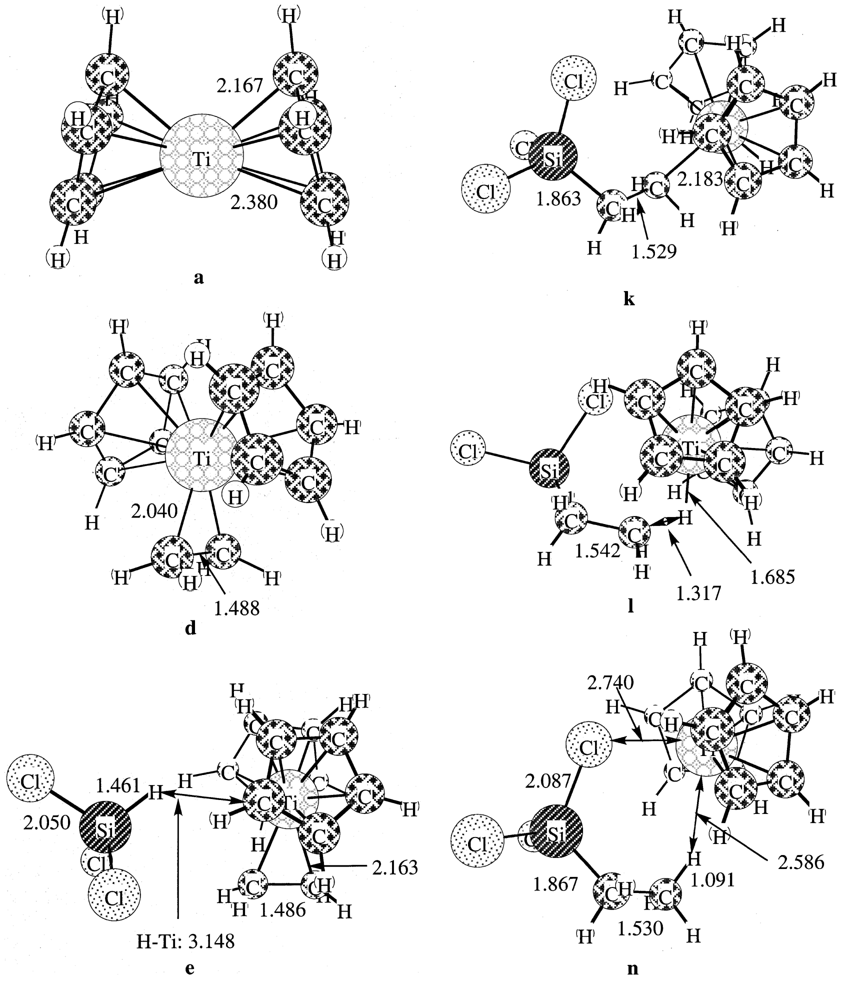

Fig. 5. MP2 structures along the minimum energy path using $TiCp_2$ as the catalyst

Table 1. MP2 relative energies (kcal/mol). The first three reactions include an MP2 ZPE correction. Those involving $TiCp_2$ are not ZPE corrected

Geometry point	**I** $TiH_2 + SiH_4 + C_2H_4$	**II** $TiH_2 + SiCl_3H + C_2H_4$	**III** $TiCl_2 + SiCl_3H + C_2H_4$	**IV** $TiCp_2 + SiCl_3H + C_2H_4$
a + **b** + **c** (reactants)	0	0	0	0
d′ + **b**	−31.1	−8.3	−10.6	
d + **c**	−61.9	−61.8	−59.6	−47.2
e	−68.4	−66.2	−64.9	−61.2
f	−66.6			
g	−66.6			
h	−61.3		−58.6	
i	−67.2	−70.0	−64.1	
j	−64.0			
k	−65.4	−74.3	−70.5	−72.1
l	−33.5	−42.3	−44.5	−42.0
m	−39.0			
n	−59.2	−46.9	−51.8	−51.4
o + **a** (products)	−28.0	−37.2	−37.2	−41.6

structure **i**, for which a reaction path has been constructed using a constrained optimization and an internal coordinate-based linear least-motion path. The highest point on this path connecting structure **e** with structure **i** is less than 6.5 kcal/mol (without ZPE correction). The second outcome shows that the transfer of a Cl from the Si to the Ti may be a competitive path to the desired reaction path. However, the mechanism for this step reduces the bond angle between the two Cl on Ti to 106° during the reaction. Since Cp rings are much larger, steric hindrance is likely to prevent this process in the mechanism of this step for the real catalyst, $TiCp_2$.

After going through the first TS the reaction proceeds to form the four-membered ring shown in **i** in Fig. 4, which is 0.8 kcal/mol above structure **e**. The four-membered ring can be opened by breaking the Si—Ti bond to give structure **k**. The barrier for the model all-hydrogen system (**I**) is 3.2 kcal/mol. Structure **k** lies 6.4 kcal/mol lower in energy than structure **j** and is the global minimum on the reaction surface at 70.5 kcal/mol below the reactants in energy. Since **k** is lower in energy than **i**, it is likely the barrier is also lower than for the model reaction (**I**). Because it is unlikely that structure **j** is qualitatively important to the overall reaction path, no attempt was made to locate it for the more complex reactions.

The final steps in the mechanism are to regenerate the catalyst by transfer of a hydrogen from Ti to C and then to eliminate the catalyst. The transition state for this process is shown in structure **l** (Fig. 4); the associated barrier height is 26.0 kcal/mol. Note, however, that this TS is still 44.5 kcal/mol lower in energy than the initial reactants.

In our previous work, the IRC for system **I** from this TS toward the products was found to proceed through a structure **m**, (not shown here), in which the catalyst is complexed to the ethylsilane product, then to a structure **n** (not shown here), in which the titanium inserts into one of the Si—H bonds. Since, for $SiCl_3H$, there are no remaining Si—H bonds. the IRC leads to the expected structure **n** (Fig. 4) with no corresponding intermediate insertion product. The complex **n** lies 7.3 kcal/mol below the TS and 14.6 kcal/mol below the seperated products in energy. From structure **n** it is quite straightforward to remove the catalyst from the complex.

Once the catalyst is removed, the process is complete with ethyltrichlorosilane as the product. The overall process is exothermic by 37.2 kcal/mol at the ZPE corrected MP2 level of theory. This compares with the value of 37.1 kcal/mol computed by Day and Gordon at the MP2/6-311G(*d,p*) level of theory.

The driving force for the entire reaction comes in the first two steps with the formation of the compound shown in structure **e** (Fig. 4), which is 64.9 kcal/mol below the reactants in energy. The reasons this structure is so stable are illustrated by the first two steps in the reaction. In the first step the electron deficient catalyst adds to the ethylene across the π bond in much the same manner as the addition of CH_2 to ethylene to form cyclopropane. The second step is much less exothermic and is driven mostly by the electrostatic attraction between the positively charged titanium (+0.47) and the negative hydrogen (−0.09) on the silicon.

4 Conclusions

The results presented here clearly show that divalent titanium is an effective catalyst for the hydrosilation reaction. All four reaction systems studied show qualitatively the same behavior. The most significant change made was the substitution of three chlorines for three hydrogens. This substitution prevented the unwanted insertion of titanium into Si—H bonds, but did not alter the qualitative aspects of the reaction path. The effect of the substituents on the titanium is smaller. While there is some change in the energetics, particularly with $TiCp_2$, there are not any qualitative changes in the main reaction path.

The overall catalyzed reaction has no net barrier, because of the very stable cyclic $TiX_2CH_2CH_2$ intermediate. However, the energy profile of the multistep process (Fig. 2) does offer the possibility of finding some of the intermediate structures if the process was carried out at low temperature.

Acknowledgements. The work described in the paper was supported by grants from the National Science Foundation (CHE-9633480) and the Air Force Office for Scientific Research (F49-620-95-1-0073). The computations were performed in part on computers provided by Iowa State University and on the CEWES T3E via the Department of Defense Grand Challenge program.

Appendix

Table A1. MP2 total energies (in Hartrees) for each reaction system

Geometry point	**II** $TiH_2 + SiCl_3H + C_2H_4$	**III** $TiCl_2 + SiCl_3H + C_2H_4$	**IV** $TiCp_2 + SiCl_3H + C_2H_4$
a	−58.582174	−87.281162	−443.436587
b	−78.317282	−78.317282	−78.317282
c	−49.032702	−49.032702	−49.032702
d′	−107.631227	−136.331341	
d	−137.002133	−165.694824	−521.829078
e	−186.043342	−214.737267	−570.884121
f			
g			
h		−214.729192	
i	−186.051765	−214.737830	
j			
k	−186.055543	−214.744744	−570.901434
l	−186.005280	−214.705339	−570.853483
m			
n	−186.017059	−214.711832	−570.868503
o	−127.416311	−127.416311	−127.416311

Table A2. MP2 zero point energy (ZPE) corrections (in Hartrees)

Geometry point	**II** $TiH_2 + SiCl_3H + C_2H_4$	**III** $TiCl_2 + SiCl_3H + C_2H_4$	**IV** $TiCp_2 + SiCl_3H + C_2H_4$
a	0.007098	0.002153	
b	0.052344	0.052344	0.052344
c	0.014483	0.014483	0.014483
d′	0.024627	0.017300	
d	0.063675	0.055931	
e	0.079623	0.071703	
f			
g			
h		0.073700	
i	0.082053	0.073437	
j			
k	0.078838	0.070207	
l	0.079660	0.072182	0.242016
m			
n	0.084093	0.077192	
o	0.073828	0.073828	0.073828

Table A3. Cartesian coordinates for each stationary point along the reaction **II**: $TiH_2 + SiH_4 + C_2H_4$

Point **a**				
Ti	22.0	0.00534	0.00000	0.00050
H	1.0	−0.12771	0.00000	1.86208
H	1.0	0.22164	0.00000	−1.85324
H	1.0	0.22164	0.00000	−1.85324
Point **b**				
C	6.0	0.00000	0.00000	0.66763
C	6.0	0.00000	0.00000	−0.66763
H	1.0	0.00000	0.92079	1.23332
H	1.0	0.00000	−0.92080	1.23329
H	1.0	0.00000	0.92079	−1.23332
H	1.0	0.00000	−0.92080	−1.23329
Point **c**				
Si	14.0	−0.01229	0.23776	0.10182
H	1.0	0.83374	1.10056	0.92945
Cl	17.0	−1.13657	−0.97774	1.31296
Cl	17.0	−1.25299	1.39974	−1.04656
Cl	17.0	1.17243	−0.91238	−1.11553
Point **d**				
Ti	22.0	0.00006	0.75244	−0.00003
C	6.0	0.74254	−1.15250	0.00010
C	6.0	−0.74310	−1.15239	−0.00002
H	1.0	0.00215	1.58254	1.53396
H	1.0	0.00036	1.58374	−1.53351
H	1.0	1.24605	−1.46977	−0.91057
H	1.0	1.24593	−1.46927	0.91101
H	1.0	−1.24654	−1.47025	0.91046
H	1.0	−1.24616	−1.46975	−0.91092
H	1.0	−1.24616	−1.46975	−0.91092
Point **d′**				
Si	14.0	−0.06888	−1.45594	1.62863
H	1.0	0.90471	−1.98251	2.57435
Cl	17.0	−1.27516	−2.94783	0.91955
Cl	17.0	−1.18898	0.08280	2.33563
Cl	17.0	0.97906	−0.77371	−0.10351
Ti	22.0	2.86347	0.70873	0.96967
H	1.0	2.26279	0.29541	2.63533
H	1.0	4.21994	1.69906	0.27382
Point **e**				
C	6.0	−3.07200	−0.20051	0.10894
C	6.0	−1.99062	0.43682	0.88915
Ti	22.0	−1.27970	−1.09680	−0.30909
H	1.0	−1.68711	1.44016	0.59816
Si	14.0	1.45240	−0.14649	1.47620
H	1.0	−3.78882	−0.81859	0.64568
H	1.0	−3.50432	0.36166	−0.71662
H	1.0	−1.98670	0.27849	1.96464
H	1.0	−1.03137	−2.66197	0.42125
H	1.0	−0.57351	−0.62287	−1.83183
H	1.0	0.71234	−0.75906	0.35403
Cl	17.0	1.39030	1.88591	1.31201
Cl	17.0	3.37257	−0.81556	1.26777
Cl	17.0	0.67809	−0.76756	3.25729
Point **i**				
C	6.0	−0.11724	−0.17349	−0.03912
C	6.0	−0.04897	0.18845	1.42051
Ti	22.0	1.93840	0.02255	−0.02548
Si	14.0	1.48128	−0.45387	2.48602
H	1.0	−0.51771	−1.15509	−0.27375
H	1.0	−0.50755	0.61211	−0.68459
H	1.0	−0.70549	−0.47571	2.00055
H	1.0	−0.28343	1.21832	1.66312
H	1.0	1.74677	−1.38923	1.08623
H	1.0	2.49748	−0.37402	−1.62265
H	1.0	1.68370	1.69274	0.14608
Cl	17.0	1.39189	−2.29278	3.43578
Cl	17.0	1.22372	0.82421	4.13596
Cl	17.0	3.48764	0.28704	1.93692
Point **k**				
C	6.0	−1.30965	1.71473	0.52557
C	6.0	−0.21767	1.70157	1.60763
Ti	22.0	−2.03525	−0.18007	0.03471
Si	14.0	1.33854	0.93571	0.92822
H	1.0	−0.98678	2.23298	−0.38479
H	1.0	−2.21081	2.22470	0.88942
H	1.0	0.02184	2.70301	1.97865
H	1.0	−0.51920	1.10870	2.47596
H	1.0	−1.94590	−0.68589	−1.59996
H	1.0	−3.72740	0.06856	0.07330
H	1.0	−1.91402	−1.30265	1.32965
Cl	17.0	0.71173	−0.75243	−0.15810
Cl	17.0	2.66826	0.31307	2.35665
Cl	17.0	2.28613	2.17659	−0.40310
Point **l**				
C	6.0	−1.31272	1.86278	0.34717
C	6.0	−0.25699	1.79850	1.47311
Ti	22.0	−1.93316	−0.35288	0.19748
Si	14.0	1.30602	0.98746	0.87682
H	1.0	−0.88488	1.92795	−0.66077

Table A3 (Contd.)

H	1.0	−1.87818	2.78978	0.46542
H	1.0	0.00306	2.79240	1.84717
H	1.0	−0.63258	1.23365	2.33371
H	1.0	−2.73058	−0.87342	−1.30169
H	1.0	−2.45708	1.22731	0.55599
H	1.0	−1.96026	−1.17915	1.77292
Cl	17.0	0.64124	−0.63243	−0.30603
Cl	17.0	2.49004	0.22544	2.35831
Cl	17.0	2.41421	2.21025	−0.33850
Point **n**				
C	6.0	−1.38645	1.86163	1.23182
C	6.0	−0.01726	1.90482	1.92068
Ti	22.0	−1.88328	−0.19186	−0.49871
Si	14.0	1.32123	0.93625	1.04343
H	1.0	−1.32421	2.02769	0.14852
H	1.0	−2.03955	2.64630	1.60954
H	1.0	0.35056	2.93152	1.97731
H	1.0	−0.09253	1.53548	2.94444
H	1.0	−1.71295	0.59498	−2.15684
H	1.0	−1.91088	0.92792	1.46639
H	1.0	−3.03941	−1.15906	0.55987
Cl	17.0	0.52623	−0.90280	0.39764
Cl	17.0	2.90746	0.52062	2.26878
Cl	17.0	1.95208	1.92404	−0.63375
Point **o**				
C	6.0	−1.93251	−0.27912	0.20303
C	6.0	−0.92943	0.77351	0.68441
Si	14.0	0.84317	0.19483	0.63693
Cl	17.0	2.10593	1.68248	1.30211
Cl	17.0	1.09415	−1.46320	1.83759
Cl	17.0	1.38576	−0.31319	−1.28689
H	1.0	−2.94731	0.11191	0.25124
H	1.0	−1.73527	−0.56964	−0.82729
H	1.0	−1.89030	−1.17509	0.81973
H	1.0	−1.13945	1.07234	1.71337
H	1.0	−0.98596	1.67627	0.07285

Table A4. Cartesian coordinates for each stationary point along the reaction **III**: $TiCl_2 + SiCl_3H + C_2H_4$

Point **a**				
Ti	22.0	0.00000	0.00000	0.00000
Cl	17.0	0.00000	0.00000	−2.30481
Cl	17.0	0.00000	0.00000	2.30481
Points **b** and **c**: same as reaction **II**				
Point **d**				
Ti	22.0	−0.35268	0.55413	0.11218
C	6.0	0.59426	−1.25311	0.08911
C	6.0	−0.87976	−1.41157	−0.03471
Cl	17.0	−0.61268	1.37473	2.16199
Cl	17.0	−0.29905	1.59111	−1.85368
H	1.0	1.19683	−1.46253	−0.79064
H	1.0	1.05469	−1.55962	1.02451
H	1.0	−1.41296	−1.82534	0.81703
H	1.0	−1.27095	−1.72750	−0.99809
Point **d′**				
Si	14.0	−0.12410	−1.61285	1.55149
H	1.0	1.01897	−1.75245	2.45042
Cl	17.0	−0.63914	−3.40625	0.72606
Cl	17.0	−1.71875	−0.74067	2.46205
Cl	17.0	0.48816	−0.36144	−0.03363
Ti	22.0	2.65739	0.82309	0.92011
Cl	17.0	1.72388	1.64867	2.86857
Cl	17.0	4.36771	−0.03160	−0.36107
Point **e**				
C	6.0	−2.36859	0.05988	−0.33220
C	6.0	−1.39767	0.56628	0.65366

Table A4 (Contd.)

Ti	22.0	−0.48768	−0.63692	−0.76586
Si	14.0	2.05543	0.27213	1.32990
H	1.0	−3.07011	−0.70579	−0.01283
H	1.0	−2.77072	0.75826	−1.06081
H	1.0	−1.14647	1.62279	0.61390
H	1.0	−1.44998	0.16571	1.66240
Cl	17.0	−0.34928	−2.79453	−0.23783
Cl	17.0	0.31916	0.44117	−2.53775
H	1.0	1.37712	−0.34758	0.17210
Cl	17.0	1.84486	2.29685	1.23775
Cl	17.0	4.01704	−0.25617	1.13254
Cl	17.0	1.28037	−0.47946	3.05774
Point **h**				
C	6.0	0.05727	0.28622	−0.00026
C	6.0	0.02531	−0.08685	1.40503
Ti	22.0	2.07181	−0.08333	0.33742
Si	14.0	1.80199	0.08318	2.94774
H	1.0	−0.32574	−0.41092	−0.73806
H	1.0	−0.09592	1.33613	−0.23870
H	1.0	−0.32238	−1.09084	1.62889
H	1.0	−0.39663	0.66444	2.05820
H	1.0	2.82176	−0.52696	1.84090
Cl	17.0	2.24247	−2.15315	−0.34083
Cl	17.0	3.31144	1.26423	−0.87918
Cl	17.0	3.43068	−0.30411	4.21476
Cl	17.0	0.30506	−0.27064	4.35789
Cl	17.0	2.03515	2.09938	2.38141
Point **i**				
C	6.0	−0.09556	0.44339	−0.09407
C	6.0	0.02572	0.65075	1.38392
Ti	22.0	1.98593	0.57074	−0.01790
Si	14.0	1.44441	−0.36820	2.33078
H	1.0	−0.51590	−0.50617	−0.40868
H	1.0	−0.47534	1.29322	−0.65651
H	1.0	−0.69532	0.02001	1.92456
H	1.0	−0.06199	1.67157	1.74388
H	1.0	1.64764	−1.01125	0.77415
Cl	17.0	2.82401	−0.38010	−1.80273
Cl	17.0	2.14744	2.79120	−0.04783
Cl	17.0	1.10512	−2.33336	2.87367
Cl	17.0	1.22900	0.58636	4.18796
Cl	17.0	3.50281	0.26847	1.96306
Point **k**				
C	6.0	−1.01178	0.79482	0.57673
C	6.0	0.20754	0.81675	1.49283
Ti	22.0	−1.89040	−0.90022	−0.18861
Si	14.0	1.75859	0.27671	0.60044
H	1.0	−0.92811	1.49174	−0.26491
H	1.0	−1.93489	1.05499	1.12994
H	1.0	0.38741	1.81790	1.89750
H	1.0	0.07352	0.14327	2.34243
Cl	17.0	−1.46207	−1.20145	−2.31707
H	1.0	−3.51770	−0.41720	−0.21022
Cl	17.0	−1.88165	−2.47109	1.34215
Cl	17.0	1.50510	−1.66363	−0.06051
Cl	17.0	3.38944	0.34764	1.84840
Cl	17.0	2.09681	1.47850	−1.03361
Point **l**				
C	6.0	−1.02175	1.06096	−0.00541
C	6.0	0.03785	1.18747	1.11145
Ti	22.0	−1.40476	−1.17583	−0.25220
Si	14.0	1.67053	0.47432	0.57303
H	1.0	−0.61000	1.22059	−1.00893
H	1.0	−1.73560	1.87765	0.12897
H	1.0	0.21298	2.23419	1.37796
H	1.0	−0.28664	0.68003	2.02247
Cl	17.0	−2.21797	−1.69496	−2.28322
H	1.0	−2.14276	0.26022	0.13275
Cl	17.0	−1.45993	−2.24628	1.73193

Table A4 (Contd.)

Cl	17.0	1.16981	−1.18650	−0.63990
Cl	17.0	2.85471	−0.21008	2.09003
Cl	17.0	2.72877	1.76578	−0.61521
Point **n**				
C	6.0	−1.08658	0.97219	0.98847
C	6.0	0.32023	1.34751	1.46932
Ti	22.0	−1.39097	−1.42504	−0.24944
Si	14.0	1.71078	0.46764	0.57771
H	1.0	−1.16744	0.94585	−0.10489
H	1.0	−1.82343	1.70335	1.31619
H	1.0	0.50236	2.41375	1.31900
H	1.0	0.42211	1.15311	2.53792
Cl	17.0	−1.44333	−0.78033	−2.46142
H	1.0	−1.40977	0.03322	1.45205
Cl	17.0	−2.27215	−2.66119	1.49039
Cl	17.0	1.17159	−1.55045	0.29388
Cl	17.0	3.44890	0.47767	1.65692
Cl	17.0	2.01335	1.26518	−1.27897
Point **o**: same as reaction **II**				

Table A5. Cartesian coordinates for each stationary point along the reaction **IV**: $TiCp_2 + SiCl_3H + C_2H_4$

Point **a**				
Ti	22.0	−0.21757	0.00009	0.00000
C	6.0	0.36857	1.16509	1.83514
C	6.0	−0.94326	0.70601	2.15400
C	6.0	−0.94323	−0.70598	2.15403
C	6.0	0.36861	−1.16502	1.83521
C	6.0	1.20367	−0.00004	−1.63631
C	6.0	0.36859	1.16504	−1.83511
C	6.0	−0.94326	0.70599	−2.15395
C	6.0	−0.94322	−0.70598	−2.15404
C	6.0	0.36863	−1.16503	−1.83527
C	6.0	1.20364	−0.00002	1.63628
H	1.0	0.69554	2.19303	1.83629
H	1.0	−1.80631	1.33202	2.33054
H	1.0	−1.80627	−1.33205	2.33058
H	1.0	0.69554	−2.19299	1.83635
H	1.0	2.27587	−0.00008	−1.52349
H	1.0	0.69560	2.19302	−1.83630
H	1.0	−1.80631	1.33200	−2.33044
H	1.0	−1.80625	−1.33207	−2.33057
H	1.0	0.69555	−2.19302	−1.83642
H	1.0	2.27586	−0.00001	1.52347
Points **b** and **c**: same as reaction **II**				
Point **d**				
Ti	22.0	−0.04818	−0.04008	−0.09574
C	6.0	0.08129	1.64853	1.62053
C	6.0	−0.87495	0.72520	2.13126
C	6.0	−0.24878	−0.53085	2.29898
C	6.0	1.11365	−0.41588	1.89531
C	6.0	1.76096	0.33292	−1.50561
C	6.0	0.91989	1.50848	−1.55819
C	6.0	−0.30929	1.13685	−2.17509
C	6.0	−0.25332	−0.23587	−2.50615
C	6.0	1.01265	−0.74916	−2.10237
C	6.0	1.33616	0.94610	1.46688
H	1.0	−0.08212	2.70287	1.46257
H	1.0	−1.92163	0.93181	2.30787
H	1.0	−0.73713	−1.43695	2.62308
H	1.0	1.86259	−1.18815	1.98083
H	1.0	2.80462	0.31010	−1.23098
H	1.0	1.20171	2.50726	−1.26577
H	1.0	−1.16587	1.78128	−2.31534
H	1.0	−1.05921	−0.80966	−2.93956
H	1.0	1.37690	−1.74814	−2.29187
H	1.0	2.29167	1.39374	1.23985
C	6.0	−1.11848	−1.77593	−0.14935
C	6.0	−2.08990	−0.65167	−0.23786
H	1.0	−1.03594	−2.39128	−1.04312
H	1.0	−1.19406	−2.41472	0.72528
H	1.0	−2.74557	−0.50738	0.61374
H	1.0	−2.61237	−0.51657	−1.17925
Point **e**				
Ti	22.0	−2.00438	0.22437	1.79736
C	6.0	−3.34441	0.58152	3.65661
C	6.0	−2.78355	−0.71125	3.82683
C	6.0	−1.38301	−0.55946	3.97732
C	6.0	−1.07208	0.81857	3.91423
C	6.0	−2.47828	2.16057	0.61569
C	6.0	−3.70225	1.43705	0.73709
C	6.0	−3.57618	0.23485	−0.00291
C	6.0	−2.28506	0.21343	−0.58166
C	6.0	−1.60705	1.40036	−0.21203
C	6.0	−2.28027	1.53303	3.70598
H	1.0	−4.39277	0.80854	3.54684
H	1.0	−3.31981	−1.64713	3.81628
H	1.0	−0.66888	−1.36061	4.07851
H	1.0	−0.08162	1.23712	3.99107
H	1.0	−2.27628	3.13417	1.03482
H	1.0	−4.57531	1.76148	1.28025
H	1.0	−4.31416	−0.54972	−0.07713
H	1.0	−1.87003	−0.58569	−1.17374
H	1.0	−0.60638	1.66515	−0.51110
H	1.0	−2.38647	2.60438	3.63666
C	6.0	−0.22429	−0.89390	1.28666
C	6.0	−1.40225	−1.79835	1.31993
H	1.0	0.21906	−0.72082	0.30987
H	1.0	0.53497	−1.05111	−2.04755
H	1.0	−1.43475	−2.52907	2.12298
H	1.0	−1.72320	−2.23321	0.37821
Si	14.0	1.86788	2.20861	1.56515
H	1.0	0.42043	2.29801	1.74296
Cl	17.0	2.68630	0.98053	2.98931
Cl	17.0	2.66626	4.09433	1.77642
Cl	17.0	2.31118	1.50604	−0.30950
Point **k**				
Ti	22.0	−1.84123	−0.57754	−1.24471
C	6.0	−1.67910	−0.15563	−3.59344
C	6.0	−0.94324	0.85728	−2.92465
C	6.0	0.14681	0.25151	−2.25691
C	6.0	0.07028	−1.14747	−2.47642
C	6.0	−1.05392	−1.39450	−3.31540
C	6.0	−1.68338	−2.82790	−0.50686
C	6.0	−2.90376	−2.68540	−1.21990
C	6.0	−3.73971	−1.79576	−0.49567
C	6.0	−3.02409	−1.37886	0.65610
C	6.0	−1.75937	−2.01957	0.65191
H	1.0	−2.56156	−0.00604	−4.19350
H	1.0	−1.19721	1.90610	−2.90301
H	1.0	0.88802	0.76080	−1.66406
H	1.0	0.76923	−1.88310	−2.11144
H	1.0	−1.36788	−2.35906	−3.68168
H	1.0	−0.84653	−3.44551	−0.79330
H	1.0	−3.15898	−3.17242	−2.14778
H	1.0	−4.74259	−1.50763	−0.76132
H	1.0	−3.38255	−0.68588	1.40143
H	1.0	−0.98243	−1.91010	1.38966
C	6.0	−1.43988	1.06705	0.13410
C	6.0	−0.90869	1.03329	1.56734
Si	14.0	0.94452	0.85941	1.63492
H	1.0	−0.98166	1.90281	−0.39652
H	1.0	−2.52653	1.27367	0.15322
H	1.0	−1.12428	1.95301	2.12695
H	1.0	−1.32571	0.21375	2.15810
H	1.0	−3.32830	0.08774	−1.84009
Cl	17.0	1.62781	−0.93472	0.85621

Table 5 (Contd.)

Cl	17.0	1.61545	0.97059	3.58695
Cl	17.0	1.85806	2.36936	0.55784
Point **l**				
C	6.0	−1.33275	1.42932	0.57876
C	6.0	−1.03008	1.27653	2.08302
Si	14.0	0.77452	1.05831	2.44121
H	1.0	−0.79342	2.29172	0.18601
H	1.0	−2.39659	1.69761	0.52764
H	1.0	−1.37648	2.15038	2.65081
H	1.0	−1.53304	0.40637	2.51049
H	1.0	−1.55300	0.69665	−0.49333
Cl	17.0	1.42515	−0.65238	1.45034
Cl	17.0	1.14445	0.78992	4.45238
Cl	17.0	1.90541	2.64625	1.77733
Ti	22.0	−0.43245	−0.55453	−0.63049
C	6.0	−0.19913	−0.35398	−2.94663
C	6.0	−0.22327	0.92883	−2.33529
C	6.0	0.93939	1.01436	−1.49221
C	6.0	1.67040	−0.20876	−1.62990
C	6.0	0.96228	−1.04630	−2.51192
C	6.0	−1.55909	−2.33921	−1.37689
C	6.0	−2.53698	−1.43875	−0.84746
C	6.0	−2.34140	−1.40504	0.56501
C	6.0	−1.25611	−2.24145	0.89354
C	6.0	−0.74054	−2.81348	−0.29912
H	1.0	−0.94611	−0.73415	−3.62532
H	1.0	−0.91594	1.72430	−2.55680
H	1.0	1.27197	1.88684	−0.95494
H	1.0	2.60322	−0.44937	−1.14562
H	1.0	1.22753	−2.06030	−2.77142
H	1.0	−1.49615	−2.67432	−2.39857
H	1.0	−3.34808	−0.97802	−1.38772
H	1.0	−2.92419	−0.82493	1.26334
H	1.0	−0.85917	−2.39098	1.88614
H	1.0	0.04892	−3.54527	−0.36639
Point **n**				
C	6.0	−1.70879	2.59619	0.11445
C	6.0	−1.01285	2.49183	1.47282
H	1.0	−1.16473	3.25563	−0.55933
H	1.0	−2.71463	2.99676	0.23963
H	1.0	−0.96288	3.47426	1.95078
H	1.0	−1.56769	1.84258	2.15321
H	1.0	−1.81066	1.62716	−0.37583
Si	14.0	0.74633	1.86543	1.46229
Cl	17.0	0.87614	−0.17510	1.04517
Cl	17.0	1.58267	2.11923	3.32857
Cl	17.0	1.89585	2.86732	0.07989
Ti	22.0	−0.95934	−0.75729	−0.90350
C	6.0	1.06229	−0.23122	−2.14385
C	6.0	0.55964	−1.48014	−2.55814
C	6.0	−0.78059	−1.27341	−3.03063
C	6.0	−1.10434	0.13224	−2.89495
C	6.0	0.06347	0.75649	−2.32771
C	6.0	−1.75633	−2.80425	−0.00456
C	6.0	−2.57337	−2.25624	−1.04706
C	6.0	−3.10863	−0.98845	−0.59688
C	6.0	−2.58519	−0.78737	0.73282
C	6.0	−1.77949	−1.90277	1.07633
H	1.0	2.03042	−0.06499	−1.69516
H	1.0	1.09743	−2.41546	−2.54159
H	1.0	−1.38193	−2.00926	−3.53701
H	1.0	−1.95175	0.63807	−3.32904
H	1.0	0.18897	1.80966	−2.13189
H	1.0	−1.22124	−3.74094	−0.03479
H	1.0	−2.85378	−2.76749	−1.95241
H	1.0	−3.90722	−0.43156	−1.06013
H	1.0	−2.82995	0.03181	1.39192
H	1.0	−1.22136	−2.01664	1.99383

Point **o** same as reaction **II**

References

1. Barton TJ, Boudjouck P (1990) In: Zieglar J, Fearon FWG (eds) Advances in silicon based polymer science. (Advances in chemistry series, no 224) American Chemical Society, Washington, pp 3–46
2. Speier JL (1979) Adv Organomet Chem 17: 407
3. Day PN, Gordon MS (1995) Theor Chim Acta 91: 83
4. Harrod JF, Ziegler T, Tschinke V (1990) Organometallics 9: 897
5. Koga N, Morokuma K (1988) J Am Chem Soc 110: 108
6. Yoshida T, Koga N, Morokuma K (1995) Organometallics 14: 746
7. Jensen VR, Børve KJ, Ystenes M (1995) J Am Chem Soc 117: 4109
8. Sakai S (1994) J Phys Chem 98: 12053
9. Kawamura-Kuribayashi H, Koga N, Morokuma K (1992) J Am Chem Soc 114: 2359
10. Stahl M, Pidun U, Frenking G (1997) Angew Chem Int Ed Engl 36: 2234
11. Bode BM, Day PN, Gordon MS (1998) J Am Chem Soc 120: 1552
12. Bode BM, Raaii F, Gordon MS (in press) In: Truhlar DG, Morokawa K (eds) Transition state modeling of catalysis in computational chemistry. (ACS symposium series no 721) American chemical Society, Washington
13. (a) For C, Si, Cl: Stevens WJ, Basch H, Krauss M (1984) J Chem Phys 81: 6026; (b) For Ti: Stevens WJ, Basch H, Krauss M, Jasien P (1992) Can J Chem 70: 612
14. The exponents used were: C $\zeta_d = 0.590$, Si $\zeta_d = 0.364$, Cl $\zeta_d = 0.566$
15. (a) For H: Ditchfield R, Hehre WJ, Pople JA (1971) J Chem Phys 54: 724; (b) For C: Hehre WJ, Ditchfield R, Pople JA (1972) J Chem Phys 56: 2257; (c) The polarization exponents, H $\zeta_p = 1.1$ and C $\zeta_d = 0.8$, are given by: Hariharan PC, Pople JA (1973) Theor Chim Acta 28: 213
16. Schmidt MW, Baldridge KK, Boatz JA, Elbert ST, Gordon MS, Jensen JH, Koseki S, Matsunaga N, Nguyen KA, Su S, Windus TL, Dupuis M, Montgomery JA Jr (1993) J Comput Chem 14: 1347
17. (a) Gonzalez C, Schlegel HB (1990) J Phys Chem 94: 5523; (b) Gonzalez C, Schlegel HB (1991) J Chem Phys 95: 5853
18. The full set of cartesian coordinates, MP2 total energies, and MP2 ZPE corrections for each structure are available as supplementary material and on the WWW site: http://www.msg.ameslab.gov/
19. Animations of the IRCs are available on the WWW site: http://www.msg.ameslab.gov/